Med Biol Eng Comput (2009) 47:641–648
DOI 10.1007/s11517-009-0473-9

ORIGINAL ARTICLE

Model-based assessment of dynamic arterial blood volume flow from ultrasound measurements

C. A. D. Leguy · E. M. H. Bosboom · A. P. G. Hoeks · F. N. van de Vosse

Received: 8 September 2008 / Accepted: 2 March 2009 / Published online: 24 March 2009

Abstract To assess in clinical practice arterial blood volume flow (BVF) from ultrasound measurements, the assumption is commonly made that the velocity profile can be approximated by a quasi-static Poiseuille model. However, pulsatile flow behaviour is more accurately described by a Womersley model. No clinical studies have addressed the consequences on the estimated dynamics of the BVF when Poiseuille rather than Womersley models are used. The aim of this study is to determine the influence of assumed Poiseuille profile instead of Womersley profile on the estimation and intrasubject variability of dynamical parameters of the BVF. For this purpose, a low number of volunteers sufficed. Brachial artery centerline velocity waveform and vessel diameter were measured with ultrasound within a small group of six volunteers. Within subjects, the intra- and inter-registration variability of BVF parameters estimates did not significantly differ. Poiseuille profiles compared to Womersley underestimates the maximum BVF by 19%, the maximum retrograde volume flow by 32% and the rise time by 18%. It can be concluded that when estimating in a straight vessel the dynamic properties of the BVF, Womersley profiles should preferably be chosen.

C. A. D. Leguy (✉) · F. N. van de Vosse
Eindhoven University of Technology,
Eindhoven, The Netherlands
e-mail: c.a.d.leguy@tue.nl

E. M. H. Bosboom
Maastricht University Medical Centre,
Maastricht, The Netherlands

A. P. G. Hoeks
Cardiovascular Research Institute Maastricht,
Maastricht University, Maastricht, The Netherlands

Keywords Blood volume flow · Brachial artery · Womersley profile · Poiseuille profile · Rise time · Ultrasound

1 Introduction

The blood pressure (BP) and blood volume flow (BVF) waveforms in large arteries are hemodynamical phenomena that result from the ejection of blood by the heart into the arterial bed [27]. The BP and BVF waveforms obtain their typical shape by superposition of a forward wave and wave reflections along the arterial tree. These reflections originate from transitions in arterial stiffness, the presence of bifurcations, arterial lumen tapering and impedance of the peripheral end segments. It has been established that arterial stiffness is an independent predictor of cardiovascular risk in an early stage [21]. Hence, the relation between arterial properties, BP and BVF waveforms has been subject of extensive analysis, using Windkessel as well as lumped parameter and wave propagation models for the arterial system (e.g. [3, 24, 32, 35]). Wave reflections have been, furthermore, investigated with several other methods such as decomposition of forward and backward traveling waves (e.g. [8, 19]). These methods require both BP and BVF waveform assessment with a high temporal resolution. Consequently, accurate in-vivo estimation of BP and BVF waveforms has become a central issue in early stage risk assessment of cardiovascular disease (CVD). This study focuses on BVF assessment. Since CVD risk assessment is part of a preventive investigation, it should be achieved by non-invasive measurement tools. For that reason, and for its high temporal resolution, ultrasound is the favorable imaging tool to determine local hemodynamic parameters in large arteries.

Ultrasound techniques, such as pulsed Doppler techniques, allow the determination of the blood velocity at a specific site [15, 23]. However, pulsed Doppler scanners have a limited spatial resolution. For peripheral applications, for instance at the brachial artery, the size of the sample volume will be of the order of 1 by 1 by 1 mm. Consequently, a Doppler registration with a sample volume located somewhere near the artery axis will easily pick up the maximum velocity which is shown as the envelope of the Doppler spectrogram. Such measurement provides the maximum "centerline" velocity although the actual position where this velocity occurred remains unknown. To extend this local measurement to the acquisition of the instantaneous blood velocity profile, sophisticated techniques such as Multi-gate-Doppler ultrasound methods have been developed [14, 38]. In these techniques, the ultrasound beam is steered with an angle of approximately 70° to the vessel wall. Consequently, a weaker reflection of the vessel wall is observed, preventing an accurate diameter measurement simultaneously and decreasing the accuracy of velocity measurements near the vessel wall. Doppler ultrasound methods have, unfortunately, some important spatial limitations due to ultrasound reflections close to the interface between the lumen and the vessel wall [22, 16]. Removal of tissue reflections by wall filtering inherently limits the ability to estimate low blood velocities. Simple integration of the acquired velocity profile is, therefore, not feasible to compute the BVF even in straight vessels with circular cross-sections.

The measurement of centerline or maximum velocity is less subject to measurement errors. In clinical studies, it is generally assumed that the velocity profile is either flat or parabolic and that the BVF is proportional to the maximum velocity waveform [10, 17, 26, 28, 30]. It is widely believed that the Womersley profile approach [41], incorporating the pulsatile behavior of the BVF, delivers more physiological waveforms than the quasi-static (parabolic) Poiseuille profile approximation. Note that both methods neglect wall movement, tapering and curvature in arteries. Although the velocity profiles given by Womersley are frequently used in computational studies [20, 36], only a few clinical studies employ this approach [33, 37]. To the authors knowledge, no clinical study has addressed the influence on the dynamics of BVF estimation when Poiseuille rather than Womersley profiles are used. Furthermore, it is not known wether inter and intra-registration variability differs between the estimates given by the two models. The goal of this study is, therefore, to investigate the influence on the shape of the BVF waveform of the quasi-static assumption using Poiseuille profiles instead of Womersley profiles and to evaluate the intra subject variability of derived parameters as rise time, and maximum and minimum peak values.

We have chosen to focus this study on the brachial artery, because it is a large artery often used for medical investigations and diagnosis [25, 43]. Furthermore, the distensibility of the brachial artery is relatively small [7, 8], unlike that of the common carotid artery [9], so the effect of wall motion on the velocity distribution is assumed to be so small that it can be neglected.

2 Materials and methods

In this study, M-mode and multi-Gate Doppler measurements are performed to determine vessel diameter and blood velocity profiles, respectively. Separate ultrasound measurement techniques are applied, because the vessel diameter cannot be accurately determined from Multi-gate Doppler measurements since the latter are not performed perpendicularly to the vessel wall. An observation angle of 70° results in a weaker and a more distributed reflection of the ultrasound beam by the vessel wall, with a different effect for the anterior and posterior wall because of opposite curvatures. In addition, an error in the assumed measurement angle induces a bias in estimated vessel diameter. Thus, the accumulated error in artery diameter may be relatively large compared to perpendicular M-mode measurement.

2.1 Assessment of vessel wall distension and maximum velocity waveforms

The ultrasonic measurements are performed using an ultrasound system (Ultramark 9 plus, Advanced Technology Laboratories, Bellevue, WA, USA). A linear array (7.5 MHz) is used in M-mode for lumen diameter assessment. The time average diameter is computed from the diameter waveform obtained with a radio-frequency acquisition system [6]. Blood velocity profiles are estimated with a broadband (5–9 MHz) curved-array transducer, activated in a wide-band M-mode with a high pulse-repetition frequency of 10 kHz [31]. A cross-correlation function is applied to short radio frequency data segments to obtain blood flow velocities [5]. Each velocity estimate is based on half overlapping data segments corresponding to 300 μm in depth and 10 ms in time. In this way, instantaneous time dependent velocity profiles along a single line of observation are obtained.

2.2 Measurement protocol

This study involved a group of six presumed healthy and non-smoking young male volunteers. Their average age was 27 years (range 21–34), their average weight 82 kg (range 69–96 kg) and their average height 1.90 m (range

1.78–2.06 m). The study was approved by the joint Medical Ethical Committee of the University of Maastricht and the Academic Hospital Maastricht and all subjects have given written informed consent. The measurements started after 10 min of rest in supine position to allow normalization of the cardiovascular function. At the start and end of the measurement session, brachial systolic and diastolic blood pressures were measured non-invasively on the left arm by means of a semi-automated oscillometric device (Dynamap, Critikon, Tampa, USA).

The location of the bifurcation of the brachial to radial and ulnar arteries of the left arm was identified in echo B-mode. To minimize the influence of this bifurcation on the velocity profile, ultrasonic measurements were performed at least 5 cm proximal. At this position, the wall distension waveform was recorded using a linear array (perpendicular approach), followed by blood flow velocity measurements using the curved array, steered at an angle of 70°. Each measurement covered four consecutive heartbeats and was repeated at least three times.

2.3 Measurements analysis

2.3.1 BVF estimation

For each volunteer, the time average of the lumen diameter $\overline{D}$ was computed from the wall distension waveform obtained in M-mode.

The time average position of the maximum velocity in an interval of 10 ms around peak systole was considered the location with peak velocity. The velocity waveform obtained at this location was called the max-line velocity V_{ml} and was used to derive the BVF. An example of the measured velocity profile and the corresponding V_{ml} is depicted in Fig. 1.

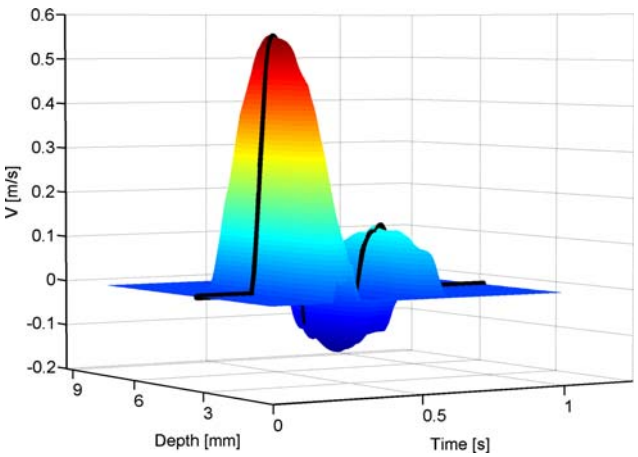

Fig. 1 An example of the velocity profile measured with ultrasound multi-gate Doppler. The *black line* shows V_{ml}

The Poiseuille BVF, q_p, was estimated by applying Poiseuille profiles on the V_{ml} waveform according to:

$$q_p(t) = \frac{\pi \overline{D}^2}{8} V_{\mathrm{ml}}(t) \tag{1}$$

In addition, the Womersley profiles BVF, q_w, was derived by applying a harmonic decomposition $\hat{V}_{\mathrm{ml}}$ of V_{ml}. The BVF results of the linear summation of flow harmonics $\hat{q}_j(t)$. Considering the temporal resolution of the Ultrasound system of 30 ms, the first 30 harmonics ($N_h = 30$) of V_{ml} were used:

$$q_w(t) = \mathrm{Real}\left(\sum_{j=1}^{N_h} \left(\hat{q}_j \exp(i\omega_j t)\right)\right) \tag{2}$$

where ω_j represents the angular frequency of each jth harmonic of V_{ml}. The harmonics $\hat{q}_j(t)$ follows from [41]:

$$\hat{q}_j = \frac{\pi \overline{D}^2}{4} G(\alpha_j) \hat{V}_{\mathrm{ml}_j}, \tag{3}$$

with:

$$G(\alpha_j) = \frac{i^{3/2}\alpha_j J_0(\alpha_j i^{3/2}) - 2J_1(\alpha_j i^{3/2})}{i^{3/2}\alpha_j J_0(\alpha_j i^{3/2}) - i^{3/2}\alpha_j}, \tag{4}$$

and:

$$\alpha_j = \frac{\overline{D}}{2}\sqrt{\omega_j / v}. \tag{5}$$

Here α denotes the Womersley number, J_i the Bessel function of order i and v the kinematic viscosity of the blood, which is the ratio between the dynamic viscosity η and the blood density ρ. In this study, η and ρ were chosen equal to 4×10^{-3}Pa.s and 1.05×10^3 kg/m^3 respectively, being standard values used in literature (e.g. [1, 2, 34]).

2.3.2 Statistical analysis

The variability of the assessed vessel diameter and the BVF waveform estimated by both Poiseuille and Womersley profiles was investigated. To evaluate the dynamic properties of BVF estimation, we considered the systolic peak BVF, the maximum backward BVF, the pulsatility index (difference between the maximum and the minimum BVF divided by the time average), and the time between the maximum and minimum BVF.

When considering a parameter X, the variability between the heartbeats of each measurement was evaluated by the intra-registration variability σ_h, which can be written as follows:

$$\sigma_h = \sqrt{\frac{\sum_v \sum_m \sum_b (X_{v,m,b} - \overline{X}_{v,m})^2}{\sum_v \sum_m (b_{v,m}) - b}} \tag{6}$$

$X_{v,m,b}$ being the parameter value for the volunteer v, in measurement m at heartbeat b, $\overline{X}_{v,m}$ the average parameter

for measurement m of volunteer v, and, $b_{v,m}$ and b being the number of heart beats of the measurement m for the volunteer v and the total number of heartbeats respectively.

The inter-registration variability σ_m that evaluates the variability between the measurements of the volunteer can be written as:

$$\sigma_m = \sqrt{\frac{\sum_v \sum_m (X_{v,m} - \overline{X}_v)^2}{\sum_v (m_v) - m}}. \quad (7)$$

In this equation, $X_{v,m}$ is the parameter value of measurement m for volunteer v and $\overline{X_v}$ the average parameter for each volunteer v. The number of measurements for the volunteer v and the total number of measurements are represented by m_v and m respectively.

The variability between the volunteers of the group was evaluated by the inter-subject variability σ_g which is defined as:

$$\sigma_g = \sqrt{\frac{\sum_v (X_v - \overline{X})^2}{v - 1}} \quad (8)$$

X_v being the parameter value for the volunteer v, $\overline{X}$ the average parameter of the group, and v the number of volunteers.

2.4 Sensitivity analysis

Both Poiseuille and Womersley profiles depend on the diameter estimated from the M-mode measurement. For Poiseuille profiles, the BVF will be proportional to the square of the diameter (Eq. 1), which corresponds to a sensitivity of order 2, meaning that a relative error in the diameter will induce a twice as high relative error in the BVF. The relation is more complex for Womersley profiles where a function $G(\alpha)$ is introduced (Eq. 1). The sensitivity of the BVF to the diameter is then of order 2 for the diameter square term plus the sensitivity of the function $G(\alpha)$. Since, the Womersley number α is proportional to the vessel diameter, the sensitivity of the function $G(\alpha)$ to the diameter equals its sensitivity, $S(\alpha)$, to α:

$$S(\alpha) = |G'(\alpha)|/\alpha \quad (9)$$

3 Results

3.1 Measurements

The diameter measurements, as depicted in Table 1, reveal a small intra-registration (±0.06 mm) and inter-registration (±0.2 mm) variability compared to the inter-subject (±0.5 mm) variability. The group average brachial diameter is equal to 4.1 mm and the group average distention is 2.7% (Table 2).

Table 1 Group average, inter-subject variability σ_g, inter-registration variability σ_m and intra-registration variability σ_h of the arterial diameter (D) and distention (ΔD) for the six volunteers

	Group average	σ_g	σ_m	σ_h
$\overline{D}$(mm)	4.1	±0.5	±0.2	±0.06
ΔD(%)	2.7	±1.4	±0.6	±0.3

Table 2 Group average, inter-subject variability σ_g, inter-registration variability σ_m and intra-registration variability σ_h of the time average, maximum (Max), minimum (Min), pulsatility index (PI) and rising time (RT) of the BVF for both Poiseuille (Poi) and Womersley (Wom) and their relative difference in %

	Group average	σ_g	σ_m	σ_h
Time average (ml/min)	27	±19	±16	±5
Max_{Wom} (ml/min)	258	±96	±40	±10
Max_{Poi} (ml/min)	204	±73	±31	±7
ΔMax (%)	−19	±2	±1	±2
Min_{Wom} (ml/min)	−72	±31	±22	±17
Min_{Poi} (ml/min)	−35	±19	±16	±11
ΔMin (%)	52	±21	±14	±12
PI_{Wom}	16	±6.1	±4.5	±1.5
PI_{Poi}	12	±4.3	±3.5	±1.1
ΔPI (%)	−26	±5.0	±2.3	±2.1
RT_{Wom} (ms)	41	±5.8	±3.0	±3.2
RT_{Poi} (ms)	48	±7.9	±2.6	±3.5
ΔRT (%)	18	±4.7	±4.8	±8.6

Of the three blood volume flow measurements for volunteer 1, only one could be used, whereas for the other volunteers at least three measurements were available. The BVF waveform estimations, displayed in Fig. 2, show that during the systolic phase the BVF quickly rises to its maximum value, then it decelerates rapidly until the flow reverses for a short time period. After this minimum, bipolar fluctuations with smaller amplitudes occur due to reflection phenomena. Large differences concerning the shape and the amplitude of these reflections are observed between the volunteers.

The time average BVF estimates are equal when considering both Poiseuille and Womersley profiles. Within each registration variation between the heartbeats is small, resulting in a small measurement standard deviation and a small intra-registration variability. The variations are larger when considering the differences between the registration for each volunteer, leading to a higher standard deviation and inter-registration variability. The time average BVF for the group is equal to 27 ml/min with an inter-registration variability of 16 ml/min, being only slightly smaller than the inter-subject variability of 19 ml/min.

Figure 3 illustrates that the group average maximum BVF equals 258 and 204 ml/min when Womersley or

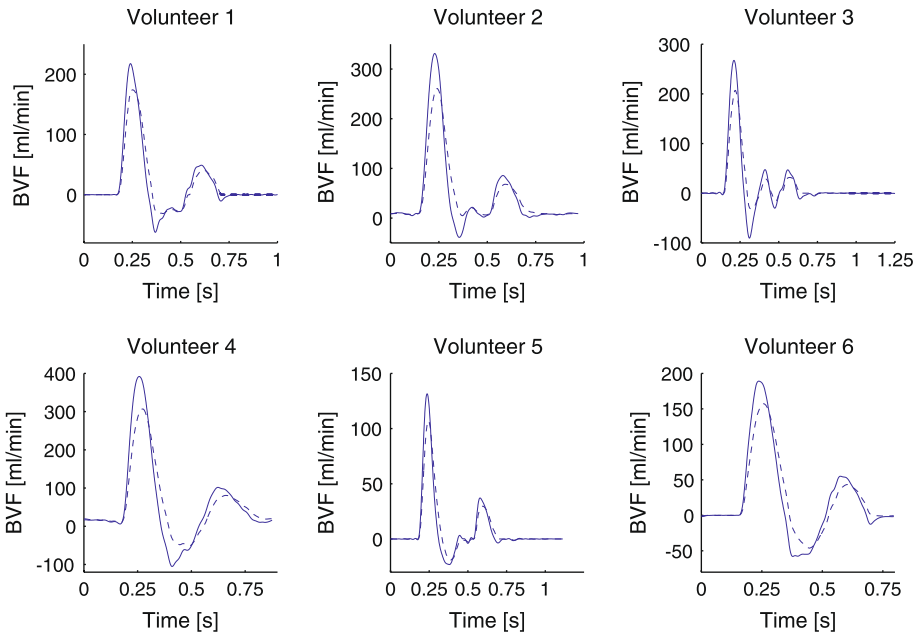

Fig. 2 Average BVF waveform obtained for each volunteer either with Poiseuille (*dashed line*) and Womersley (*straight line*)

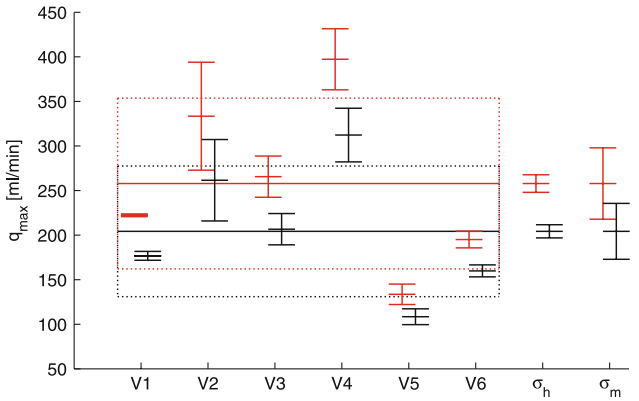

Fig. 3 Maximum BVF was estimated by Poiseuille and Womersley. In this figure, ∓ denotes subject average and standard deviation, ⋯⋯ denotes group average and inter-subject variability, *black line* represents Poiseuille and *red line* represents Womersley. σ_h and σ_m represent intra- and inter-registration variabilities, respectively. V1,…, V6 denote volunteer 1,…, volunteer 6, respectively.

Poiseuille are used, respectively. Compared to Womersley BVF estimation, Poiseuille BVF estimation underestimates the maximum BVF thus by 19%. For both methods, a smaller intra-registration (±10 ml/min for Womersley and ±7 ml/min for Poiseuille) than inter-registration variability (±40 ml/min for Womersley and ±31 ml/min for Poiseuille) is observed, whereas the inter-registration variability is almost a factor of two lower than the inter-subject variability (±96 ml/min for Womersley and ±73 ml/min for Poiseuille).

A difference of 52% is observed between estimation of the minimum BVF with Womersley (72 ml/min) and Poiseuille (35 ml/min) profiles. When using Poiseuille profiles the maximal backflow is underestimated. The registration standard deviation is quite large, resulting in a slightly lower intra-registration variability, ±17 ml/min for Womersley and ±11 ml/min for Poiseuille, than the inter-registration variability, ±22 ml/min for Womersley and ±16 ml/min for Poiseuille. The latter is lower than the group variability which equals ±31 ml/min for Womersley and ±19 ml/min for Poiseuille. The larger variability observed for the minimum BVF, compared to the one obtained for the maximum BVF, is because the retrograde velocities (0.1–0.3 m/s) is small compared to the resolution of the ultrasound Doppler machine.

The group average of the pulsatility index underestimated by 26% by Poiseuille compared to Womersley, as the estimates equal 12 and 16, respectively. The intra-registration (±1.5 for Womersley and ±1.1 for Poiseuille) and inter-registration variability (±4.5 for Womersley and ±3.5 for Poiseuille) are lower than the intersubject variability (±6.1 for Womersley and ±4.3 for Poiseuille).

Figure 4 displays the estimates for the rise time, being of 41 and 48 ms for Womersley and Poiseuille, respectively. Poiseuille thus underestimates the rise time by 18%. A slightly larger intra-registration (±3.2 for Womersley and ±3.5 ms for Poiseuille) than inter-registration variability (±3.0 for Womersley and ±2.6 ml/min for Poiseuille) is observed demonstrating a large beat-to-beat variation. On other hand, the inter-registration variability is a factor two lower than the inter-subject variability (±5.8 ms for Womersley and ±7.9 ms for Poiseuille).

3.2 Sensitivity analysis

For the physiological range of α, below 20, the sensitivity function $S(\alpha)$ remains smaller than 0.1 (Fig. 5). It can thus

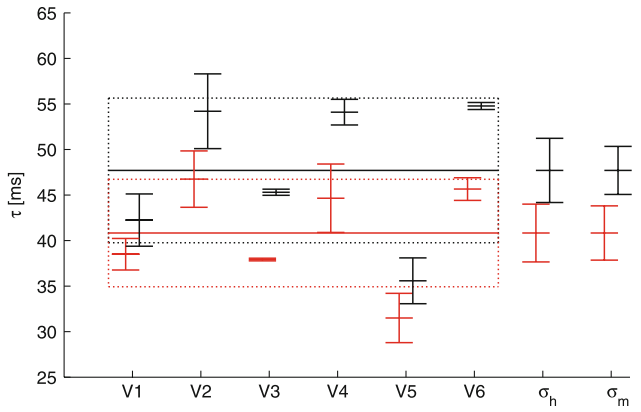

Fig. 4 Rise time was estimated by Poiseuille and Womersley. In this figure, ∓ denotes subject average and standard deviation, ⎓ denotes group average and inter-subject variability, *black line* represents Poiseuille and *red line* represents Womersley. σ_h and σ_m represent intra- and inter-registration variabilities, respectively. V1,…, V6 denote volunteer 1,…, volunteer 6, respectively

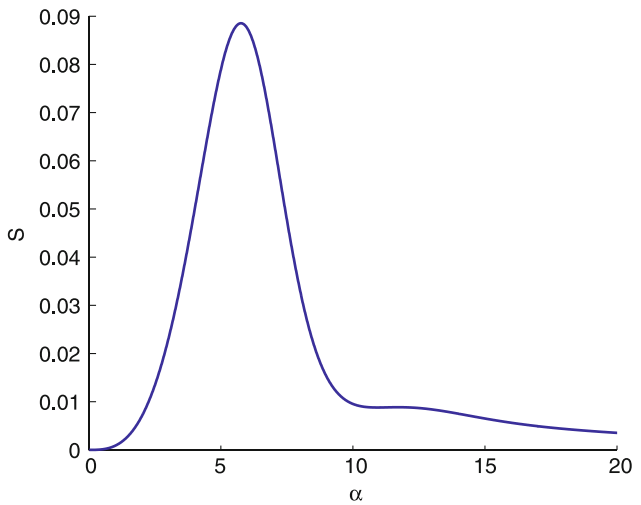

Fig. 5 The sensitivity function $S(\alpha)$ as function of the Womersley parameter α

be concluded that the diameter sensitivity of the Womersley and Poiseuille methods to estimate BVF from centerline velocity is slightly higher than and equal to order 2, respectively.

4 Discussion

In this study, the influence of assuming quasi-static Poiseuille profiles has been investigated for the BVF waveform of the brachial artery. In the present study, we focus on the reproducibility within subjects, so a low number of volunteers sufficed. However, for a comparison of parameters between groups a larger population is required. The results show that using Poiseuille induces a large bias in estimates reflecting the dynamical properties of the BVF waveform. High resolution techniques are required to accurately retrieve the BVF waveform shape because of its short rise time, a requirement only Womersley can comply with.

The brachial velocity waveforms considered in this study correspond to waveforms found in literature (e.g. [9, 13, 33]). Considering the group mean BVF, the value obtained in this study is comparable to the value of 30.6 ml/min reported by Green [13] for a group of healthy volunteers at rest conditions.

The differences in the dynamical parameters obtained by assuming Poiseuille rather than Womersley profiles can be explained by the shape of the BVF waveform. During the systolic part, the acceleration of the blood is very fast which results into a flat profile. Using a parabolic profile instead of the Womersley approximation underestimates the volume flow and its derivative. Consequently, the rise time as well as the maximum value are underestimated. During the deceleration part, the velocity profiles tend to be more parabolic, thus the difference between Womersley and Poiseuille estimates will be smaller. During the more constant parts of the BVF waveform, corresponding to a low Womersley number, the quasi-static Poiseuille profiles and Womersley profiles converge.

In this paper, the mean diameter, measured in M-mode, was used together with the max-line velocity waveforms as measured with multi-gate Doppler, to estimate the BVF. The variability of the diameter measurements influences significantly the accuracy of BVF estimation. A more accurate BVF estimation could be obtained if both vessel diameter and blood velocity are measured simultaneously. Such a technique would allow to obtain the BVF waveform on a beat-to-beat basis. Furthermore, if the velocity profile can be measured accurately along a single line, the integration of the profile would allow direct estimation of the BVF, while it would take into account the movement of the vessel wall as well as the influence of non-Newtonian blood properties on the shape of the velocity profile. Beulen et al. have validated such technique, using a commercially available ultrasound scanner equipped with a linear array probe, by comparing axial velocity profile measurements in a phantom setup to analytical and computational fluid dynamics calculations [4].

Both Poiseuille and Womersley theory (in the form used in this study) assume non moving vessel walls. Since the distension of the brachial artery is small (2.8%), it will have only little influence on the estimation of the BVF. Nonetheless, in larger and more elastic arteries, such as the common carotid artery, vessel-wall movement could have a significant influence on BVF estimation. Therefore, the results of this study cannot be transposed directly to such arteries. Unfortunately, no theoretical model exists for

moving-wall tubes without knowing the pressure gradient [41]. However, computational fluid dynamics (CFD) could be utilized to quantify the BVF estimation error introduced by the movement of the vessel wall and to investigate how BVF estimation could be improved (for this purpose, an estimate of either the mechanical properties or the vessel wall distension and blood pressure would be necessary).

Both Poiseuille and Womersley expansions are based on velocity profiles in straight arteries. However, most arteries are curved. CFD (e.g. [12, 29, 42]) and analytical studies (e.g. [11, 40]) have shown that vessel curvature can have a strong influence on the shape of the velocity profile. The analytical models proposed by Waters et al. are interesting but, however, limited to steady flow for low Dean numbers, which does not correspond to physiological flow [40]. Nevertheless, Verkaik et al. demonstrated using CFD that the analytical solution can be extended to higher Dean numbers [39]. Thus, the use of either Poiseuille or Womersley profiles in vivo involves an estimation error. As in curved tubes Womersley theory is not valid anymore, CFD simulations in curved tubes or analytical solutions involving physiological BVF waveforms should be used to evaluate the errors in the BVF estimation. The feasibility of alternative methods to accurately estimate the BVF in curved arteries has been investigated [39].

In this study, it has been shown that using Poiseuille instead of Womersley profiles incurs large errors in the estimation of the dynamical properties of the BVF and it is thus important to realize its consequences. However, nowadays common clinical diagnosis of cardiovascular diseases is still mainly based on blood pressure estimation: the bias of dynamic BVF parameters thus has only limited consequences. If we are considering the Pressure–Velocity loop method, based on both blood pressure and volume flow waveforms during the early systole in order to estimate pressure wave speed, as developed by Khir and Parker [18], an error in the BVF rise time estimate of 18% and in the maximum of 19% results in an overestimation of the pressure wave speed in the order of 35%. Furthermore, the bias in the BVF dynamics parameters influences significantly cardiovascular research studies involving better modeling and understanding of the cardiovascular biomechanics. For instance, models like windkessel, lumped parameters, wave propagation or 3D fluid dynamics models are based on dynamical BVF waveforms [3, 24, 32, 35].

5 Conclusion

Although it is widely believed that the Womersley profile approach delivers more physiological waveforms than the Poiseuille profiles approximation, it is rarely used in clinical studies despite the fact that Bessel functions are presently available for standard software packages like Excel (Microsoft) or Matlab (The Mathworks) and could readily be implemented on ultrasound systems. The time average BVF and the variability of the dynamic parameters are similar using Poiseuille or Womersley approach, whereas the influence of using Poiseuille rather than Womersley profiles on the estimated BVF waveform has never been reported. We have shown that for physiological blood velocity waveforms the dynamic characteristics of the BVF derived using Poiseuille are strongly biased. Poiseuille profiles compared to Womersley underestimate the maximum BVF by 19%, the maximum retrograde flow by 32% and the rise time by 18%, implying a significant bias for clinical methods involving BVF waveforms.

Acknowledgments This research has been supported by a Marie Curie Early Stage Research Training Fellowship of the European Community's Sixth Framework Programme under contact number MEST-CT-2004-514421.

References

1. Amornsamankul S, B. W. amd Y. H. Wu, Lenbury Y (2006) Effect of non-newtonian behavior of blood on pulsatile flows in stenotic arteries. Int J Biomed Sci 1:1306–1216
2. Benard N, Perrault R, Coisne D (2006) Computational approach to estimating the effects of blood properties on changes in intra-stent flow. Ann Biomed Eng 34:1259–1271
3. Bessems D, Rutten M, Vosse F (2007) A wave propagation model of blood flow in large vessels using an approximate velocity profile function. J Fluid Mech 580:145–168
4. Beulen BWA, Rutten M, Vosse FN (2009) Perpendicular ultrasound velocity measurement by cross correlation of rf data: experiments and validation. Ultrasound Med Biol (submitted)
5. Brands PJ, Hoeks AP, Hofstra L, Reneman RS (1995) A noninvasive method to estimate wall shear rate using ultrasound. Ultrasound Med Biol 21:171–185
6. Brands PJ, Hoeks AP, Ledoux LA, Reneman RS (1997) A radio frequency domain complex cross-correlation model to estimate blood flow velocity and tissue motion by means of ultrasound. Ultrasound Med Biol 23:911–920
7. Budoff MJ, Flores F, Tsai J, Frandsen T, Yamamoto H, Takasu J (2003) Measures of brachial artery distensibility in relation to coronary calcification. Am J Hypertens 16:350–355
8. Dammers R, Tordoir JHM, Hameleers JMM, Kitslaar PJEHM, Hoeks APG (2002) Brachial artery shear stress is independent of gender or age and does not modify vessel wall mechanical properties. Ultrasound Med Biol 28:1015–1022
9. Dammers R, Stifft F, Tordoir JHM, Hameleers JMM, Hoeks APG, Kitslaar PJEHM (2003) Shear stress depends on vascular territory: comparison between common carotid and brachial artery. J Appl Physiol 94:485–489
10. Davies JE, Whinnett ZI, Francis DP, Willson K, Foale RA, Malik IS, Hughes AD, Parker KH, Mayet J (2006) Use of simultaneous

pressure and velocity measurements to estimate arterial wave speed at a single site in humans. Am J Physiol Heart Circ Physiol 290:H878–H885
11. Dean W (1928) The stream-line motion of fluid in a curved pipe. Philos Mag 5:673–695
12. Gijsen FJ, Allanic E, van de Vosse FN, Janssen JD (1999) The influence of the non-newtonian properties of blood on the flow in large arteries: unsteady flow in a 90 degrees curved tube. J Biomech 32:705–713
13. Green D, Cheetham C, Reed C, Dembo L, O'Driscoll G (2002) Assessment of brachial artery blood flow across the cardiac cycle: retrograde flows during cycle ergometry. J Appl Physiol 93:361–368
14. Hoeks A, Reneman R, Peronneau P (1981) A multi-gate pulsed doppler system with serial data processing. IEEE Trans Sonics Ultrason SU-28:242–247
15. Hoeks AP, Ruissen CJ, Hick P, Reneman RS (1984) Methods to evaluate the sample volume of pulsed doppler systems. Ultrasound Med Biol 10:427–434
16. Hoeks AP, Hennerici M, Reneman RS (1991) Spectral composition of doppler signals. Ultrasound Med Biol 17:751–760
17. Holdsworth DW, Norley CJ, Frayne R, Steinman DA, Rutt BK (1999) Characterization of common carotid artery blood-flow waveforms in normal human subjects. Physiol Meas 20:219–240
18. Khir AW, Parker KH (2005) Wave intensity in the ascending aorta: effects of arterial occlusion. J Biomech 38:647–655
19. Khir AW, O'Brien A, Gibbs JS, Parker KH (2001) Determination of wave speed and wave separation in the arteries. J Biomech 34:1145–1155
20. Kirpalani A, Park H, Butany J, Johnston KW, Ojha M (1999) Velocity and wall shear stress patterns in the human right coronary artery. J Biomech Eng 121:370–375
21. Laurent S, Cockcroft J, Bortel LV, Boutouyrie P, Giannattasio C, Hayoz D, Pannier B, Vlachopoulos C, Wilkinson I, Struijker-Boudier H, European Network for Non-invasive Investigation of Large Arteries (2006) Expert consensus document on arterial stiffness: methodological issues and clinical applications. Eur Heart J 27:2588–2605
22. Ledoux LA, Brands PJ, Hoeks AP (1997) Reduction of the clutter component in doppler ultrasound signals based on singular value decomposition: a simulation study. Ultrason Imaging 19:1–18
23. Levenson JA, Peronneau PA, Simon A, Safar ME (1981) Pulsed doppler: determination of diameter, blood flow velocity, and volumic flow of brachial artery in man. Cardiovasc Res 15:164–170
24. Matthys KS, Alastruey J, Peiró J, Khir AW, Segers P, Verdonck PR, Parker KH, Sherwin SJ (2007) Pulse wave propagation in a model human arterial network: assessment of 1-d numerical simulations against in vitro measurements. J Biomech 40(15):3476–3486
25. Michel E, Zernikow B (1998) Gosling's doppler pulsatility index revisited. Ultrasound Med Biol 24:597–599
26. Mitchell GF, Parise H, Vita JA, Larson MG, Warner E, Keaney JF, Keyes MJ, Levy D, Vasan RS, Benjamin EJ (2004) Local shear stress and brachial artery flow-mediated dilation: the framingham heart study. Hypertension 44:134–139
27. Nichols W, O'Rourke M (2005) McDonald's blood flow in arteries, 5th ed. Hodder Arnold, London
28. Parker KH, Jones CJ (1990) Forward and backward running waves in the arteries: analysis using the method of characteristics. J Biomech Eng 112:322–326
29. Perktold K, Nerem RM, Peter RO (1991) A numerical calculation of flow in a curved tube model of the left main coronary artery. J Biomech 24:175–189
30. Safar ME, Peronneau PA, Levenson JA, Toto-Moukouo JA, Simon AC (1981) Pulsed doppler: diameter, blood flow velocity and volumic flow of the brachial artery in sustained essential hypertension. Circulation 63:393–400
31. Samijo SK, Willigers JM, Brands PJ, Barkhuysen R, Reneman RS, Kitslaar PJ, Hoeks AP (1997) Reproducibility of shear rate and shear stress assessment by means of ultrasound in the common carotid artery of young human males and females. Ultrasound Med Biol 23:583–590
32. Segers P, Rietzschel ER, Buyzere MLD, Vermeersch SJ, Bacquer DD, Bortel LMV, Backer GD, Gillebert TC, Verdonck PR, and A. investigators (2007) Noninvasive (input) impedance, pulse wave velocity, and wave reflection in healthy middle-aged men and women. Hypertension 49:1248–1255
33. Simon AC, Flaud P, Levenson J (1990) Non-invasive evaluation of segmental pressure drop and resistance in large arteries in humans based on a poiseuille model of intra-arterial velocity distribution. Cardiovasc Res 24:623–626
34. Simon AC, Levenson J, Flaud P (1990) Pulsatile flow and oscillating wall shear stress in the brachial artery of normotensive and hypertensive subjects. Cardiovasc Res 24:129–136
35. Stergiopulos N, Westerhof BE, Westerhof N (1999) Total arterial inertance as the fourth element of the windkessel model. Am J Physiol 276:H81–H88
36. Stroev PV, Hoskins PR, Easson WJ (2007) Distribution of wall shear rate throughout the arterial tree: a case study. Atherosclerosis 191:276–280
37. Struijk PC, Stewart PA, Fernando KL, Mathews VJ, Loupas T, Steegers EAP, Wladimiroff JW (2005) Wall shear stress and related hemodynamic parameters in the fetal descending aorta derived from color doppler velocity profiles. Ultrasound Med Biol 31:1441–1450
38. Tortoli P, Guidi F, Guidi G, and A. C (1996) Spectral velocity profiles for detailed ultrasound flow analysis. IEEE Trans Ultrason Ferroelectr Freq Control 43:654–658
39. Verkaik AC, Beulen BWAMM, Bogaerds ACB, Rutten MCM, van de Vosse FN (2009) Estimation of volume flow in curved tubes based on analytical and computational analysis of axial velocity profiles. Phys Fluids 21:023602
40. Waters SL, Pedley TJ (1999) Oscillatory flow in a tube of time-dependent curvature. part 1. perturbation to flow in a stationary curved tube. J Fluid Mech 383:353–378
41. Womersley J (1957) An elastic tube theory of pulse transmission and oscillatory flow in mammalian arteries. Technical report WADC-TR-56-614
42. Yao H, Ang KC, Yeo JH, Sim EK (2000) Computational modelling of blood flow through curved stenosed arteries. J Med Eng Technol 24:163–168
43. Yufu K, Takahashi N, Anan F, Hara M, Yoshimatsu H, Saikawa T (2004) Brachial arterial stiffness predicts coronary atherosclerosis in patients at risk for cardiovascular diseases. Jpn Heart J 45:231–242